Electronic Supplementary Material (ESI) for Physical Chemistry Chemical Physics.

Electronic Supplementary Information

A regulation strategy of self-assembly molecules for achieving efficient inverted perovskite solar cells

Pu-An Lin[a, b, c], Bo Yang[a, b], Changqing Lin[d], Zhenghui Fan[a, b], Yu Chen[e], Wenfeng Zhang[f], Bing Cai[c*], Jie Sun[a*], Xiaojia Zheng[a, b], Wen-Hua Zhang[c*]

[a] Institute of Chemical Materials, China Academy of Engineering Physics, Mianyang 621900, China.

[b] National Energy Novel Materials Center, Chengdu 610200, China.

[c] Yunnan Key Laboratory of Carbon Neutrality and Green Low-carbon Technologies, School of Materials and Energy, Yunnan University, Kunming, Yunnan 650000, China.

[d] School of Physical Science and Technology, Guangxi University, Nanning 530004, China.

[e] College of Materials and Chemistry & Chemical Engineering, Chengdu University of Technology, Chengdu, 610059 P. R. China.

[f] Institute of Photovoltaic, Southwest Petroleum University, Chengdu, 610500, China.

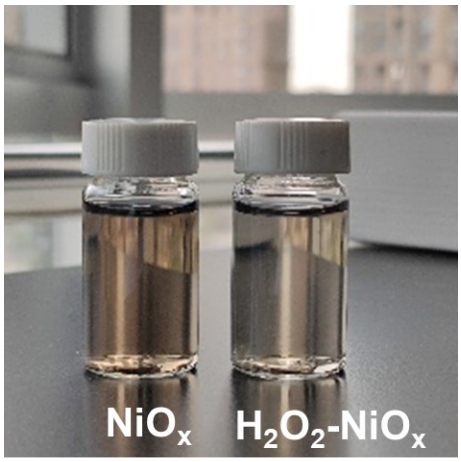

Supplementary Fig. 1. Photos of NiO_x aqueous solution (left) and H_2O_2-NiO_x aqueous solution (right) with 2 mg mL^{-1}.

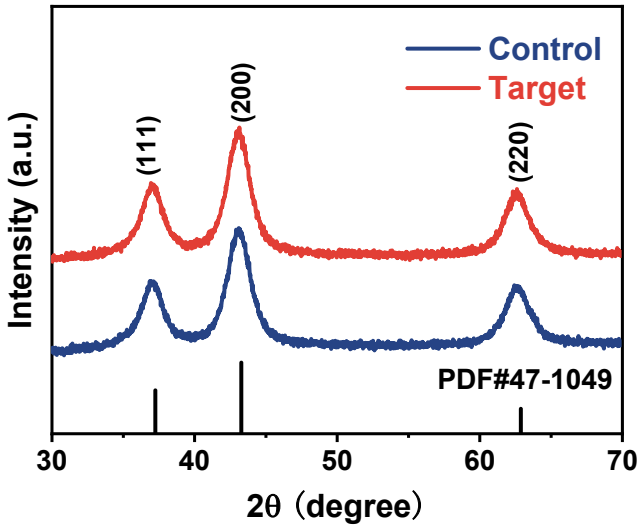

Supplementary Fig. 2. XRD patterns of the control and target NiO_x NCs powders.

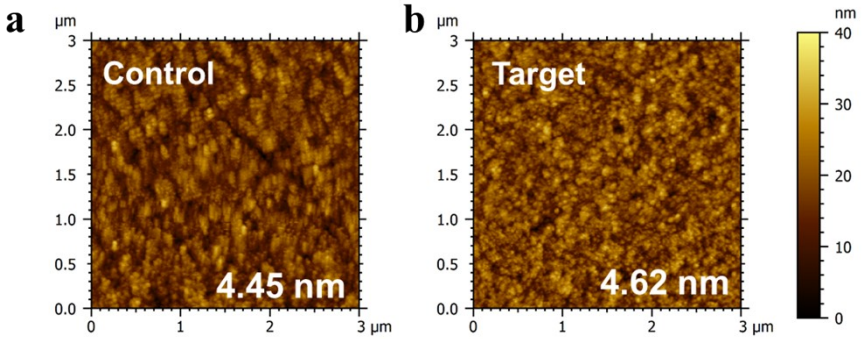

Supplementary Fig. 3. (a-b) AFM images of NiO_x film from the control sample (a) and target sample (b). The numerical values in the bottom right of the figure represent the root mean square (RMS) roughness of the NiO_x films. The RMS for the control sample is 4.62 nm, while the RMS for the target sample is 4.62 nm.

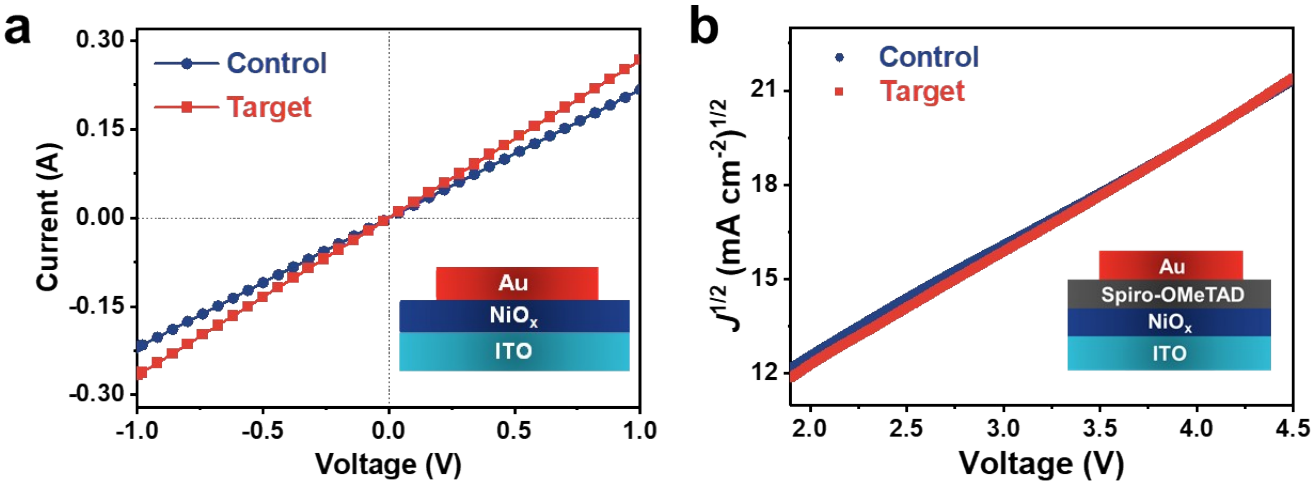

Supplementary Fig. 4. (a) The current-voltage (I-V) plots of the control and target NiO_x films with a configuration of ITO/NiO_x/Au. (b) Hole mobility of the control and target NiO_x films with a configuration of ITO/NiO_x/Spiro-OMeTAD/Au.

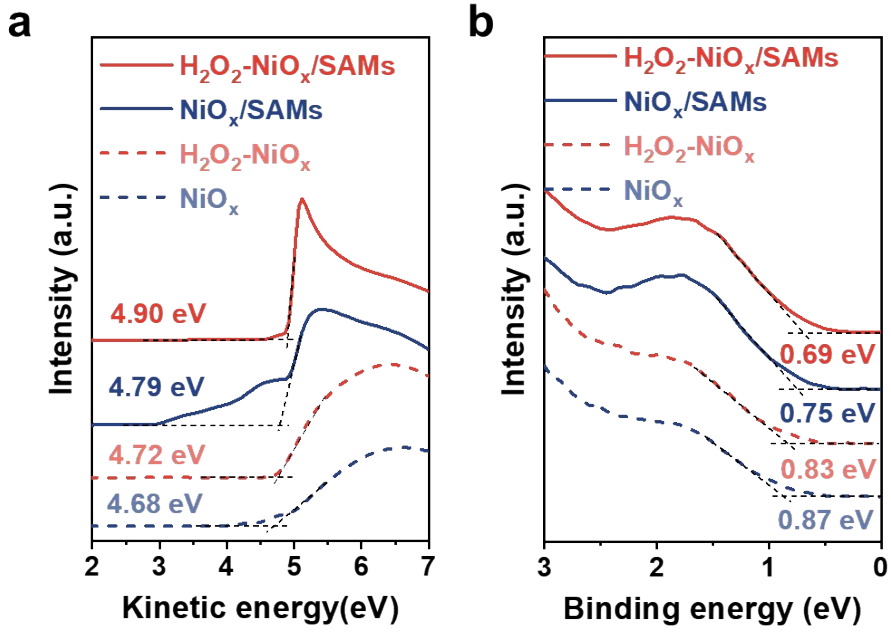

Supplementary Fig. 5. UPS spectra of ITO substrates covered by NiO_x, H_2O_2-NiO_x, NiOx/SAMs, H_2O_2-NiO_x/SAMs. (a) The secondary electron cut-off regions of UPS spectra. (b) Valence band onset regions of UPS spectra.

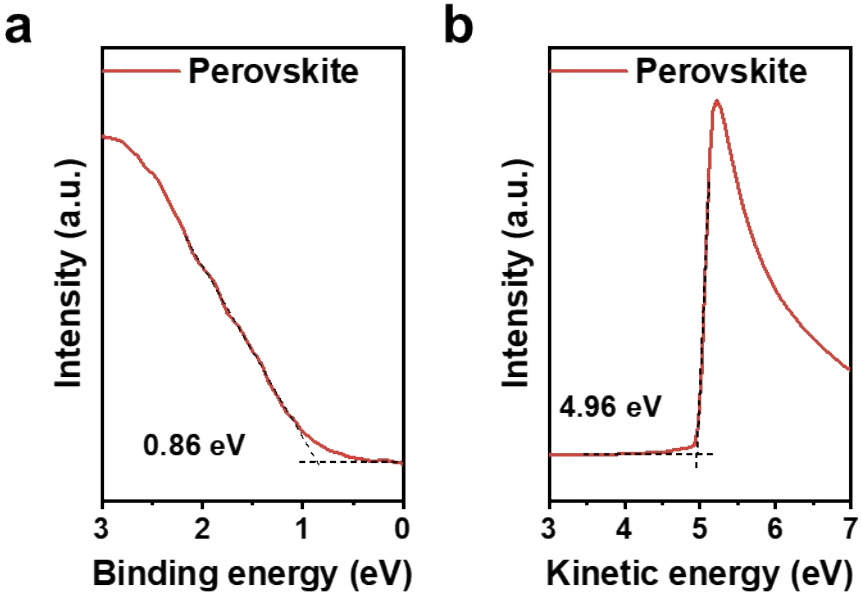

Supplementary Fig. 6. UPS spectra of perovskite film based on ITO substrate. (a) Valence band onset regions of UPS spectra. (b) The secondary electron cut-off regions of UPS spectra.

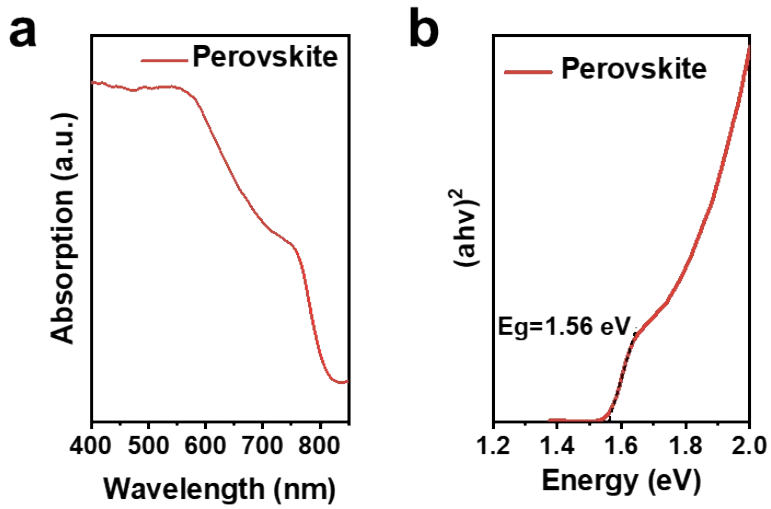

Supplementary Fig. 7. (a) The UV-vis absorption spectra of perovskite film. (b) Tauc plot of the perovskite film extracted from UV-vis absorption spectra.

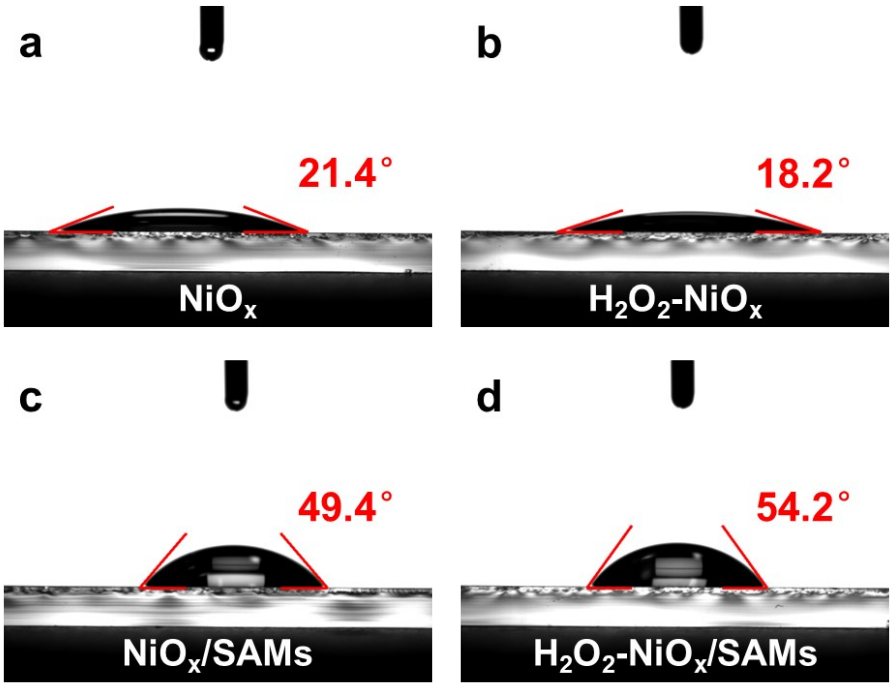

Supplementary Fig. 8. Contact angles of (a) NiO_x, (B) H_2O_2-NiO_x, (C) NiO_x/SAMs and (D) H_2O_2-NiO_x /SAMs with respect to water.

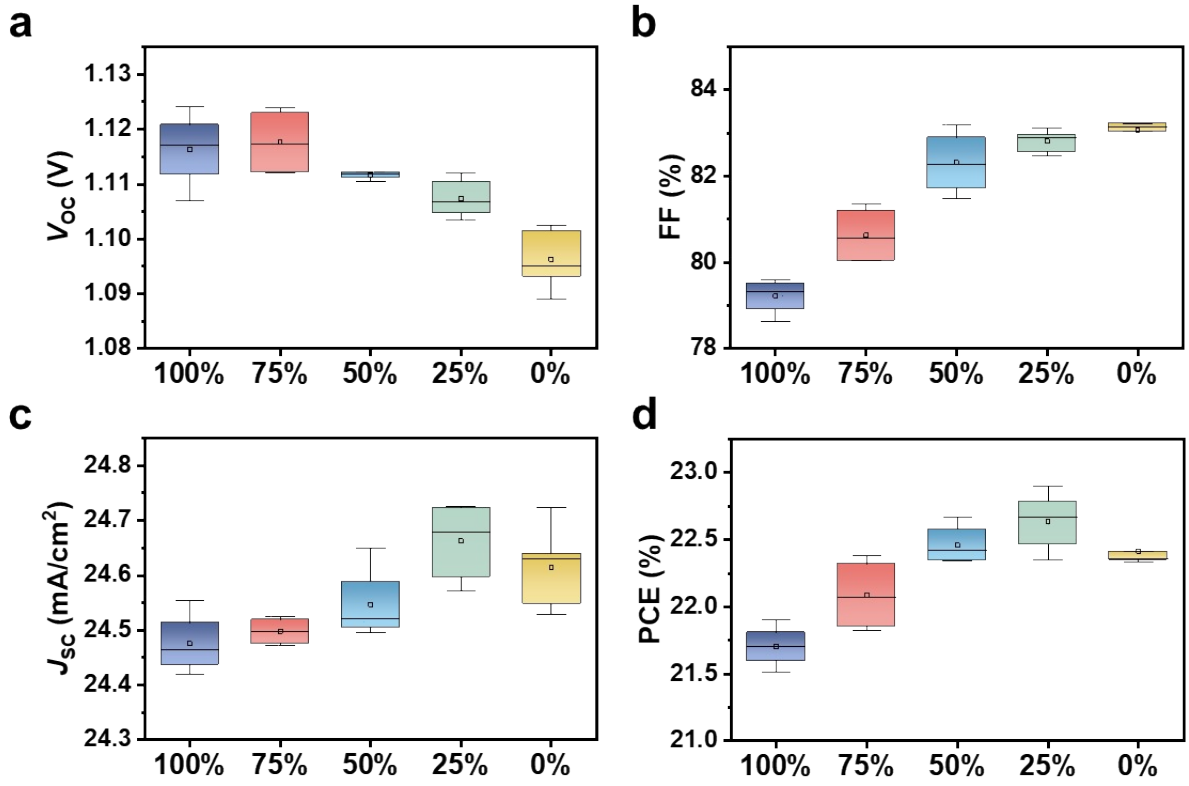

Supplementary Fig. 9. The statistics of performance parameters of p-i-n devices based on H_2O_2-NiO_x substrate with various molar ratios of MeO-2PACz in mixed SAMs.

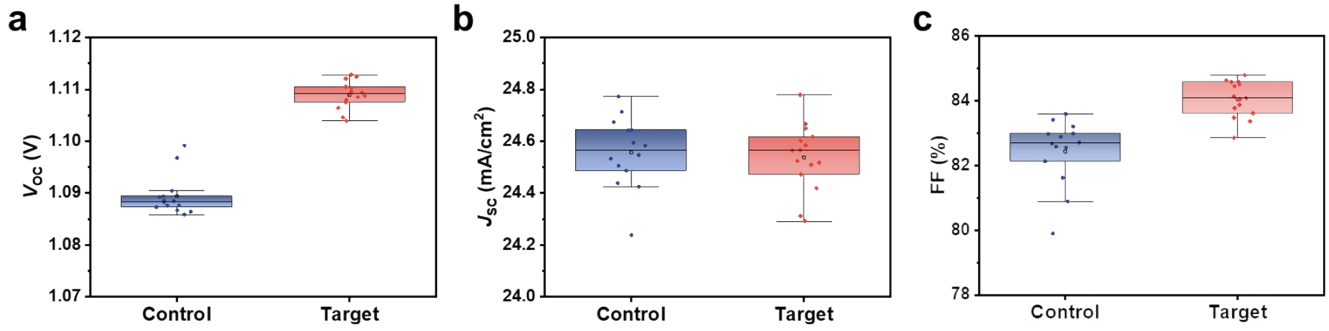

Supplementary Fig. 10. The statistics of performance parameters of p-i-n devices based on different HTLs. (a) Open-circuit voltage (V_{OC}), (b) short circuit current density (J_{SC}), (c) fill factor (FF).

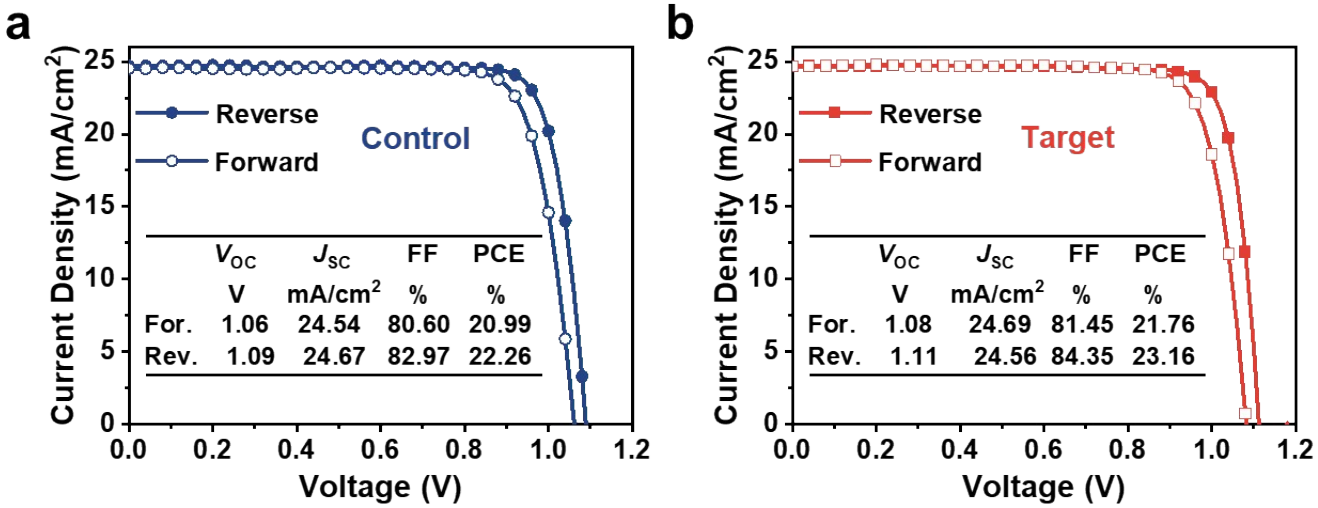

Supplementary Fig. 11. J-V curves of best-performing (a) control device and (b) target device obtained in forward and reverse scans with an aperture area of 0.09 cm^2.

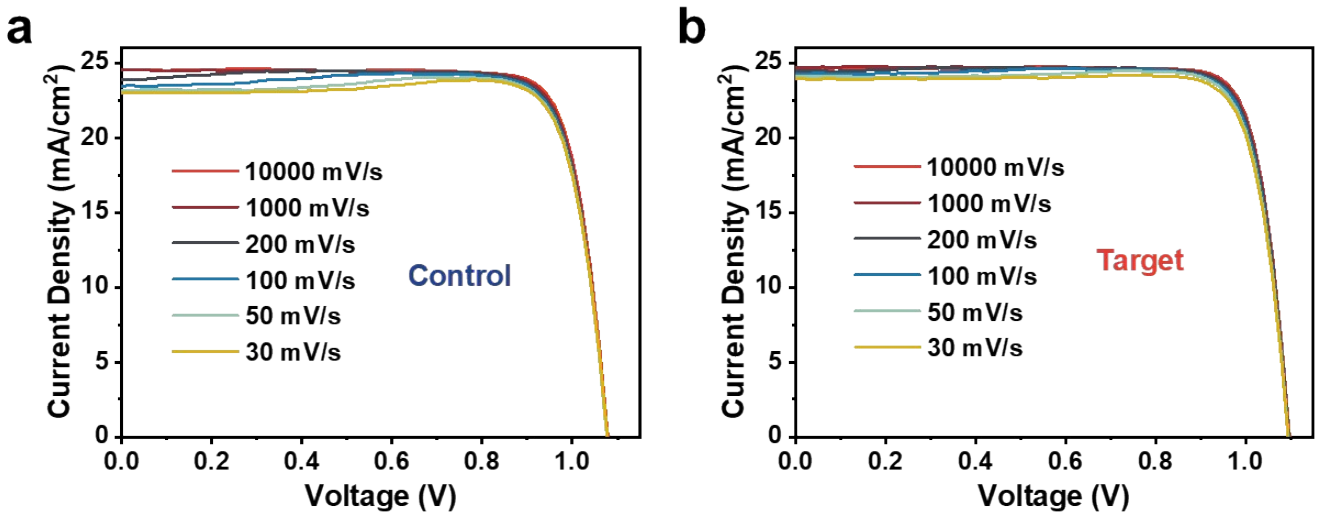

Supplementary Fig. 12. J-V curves of PSCs with different sweep rates from 30 to 10000 mV s^{-1} in reverse scans, with an aperture area of 0.09 cm^2.

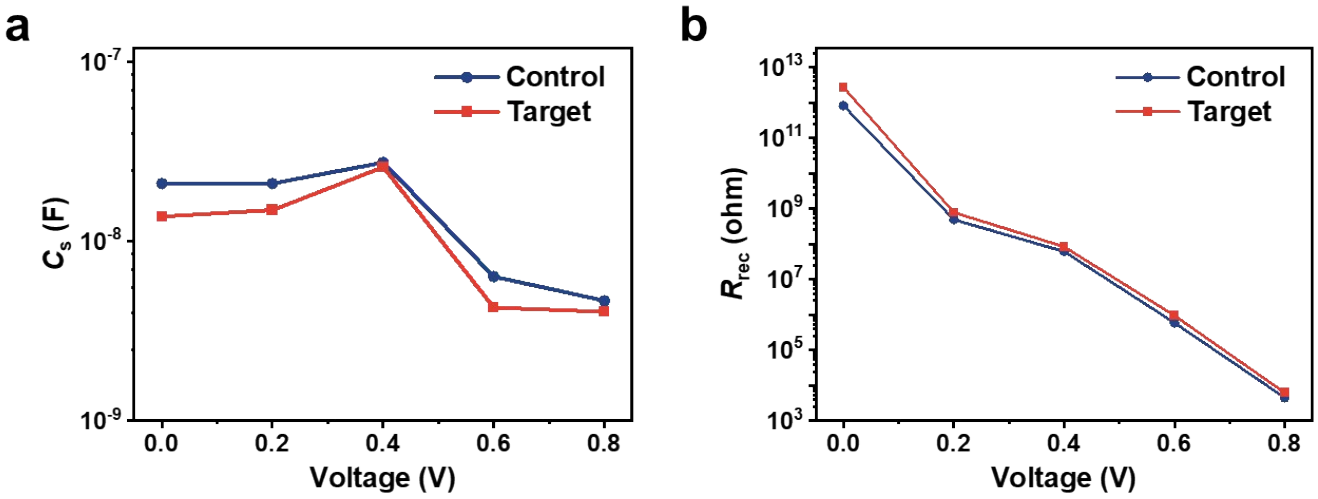

Supplementary Fig. 13. Electrochemical impedance spectroscopy (EIS) measurements of the control and target devices. C_S (a) and R_{rec} (b) as a function of the bias-voltage of PSCs.

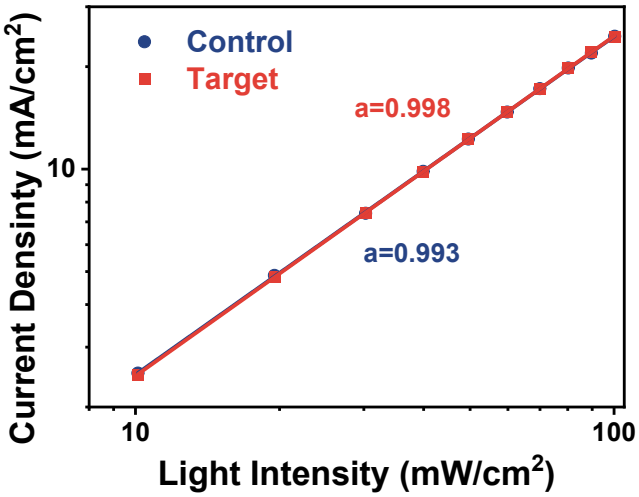

Supplementary Fig. 14. Dependence of J_{SC} versus the irradiation intensity for the control and target devices.

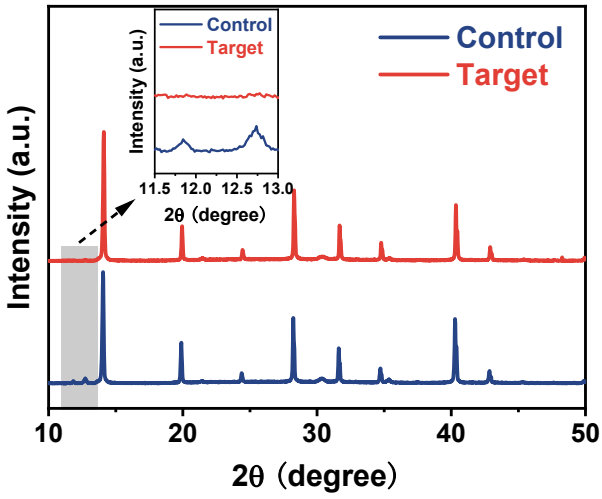

Supplementary Fig. 15. The XRD patterns of the perovskite film after 1500 h in a controlled chamber with 40% relative humidity. The grey area is the signal of perovskite degradation with the appearance of some PbI_2 diffraction peaks.

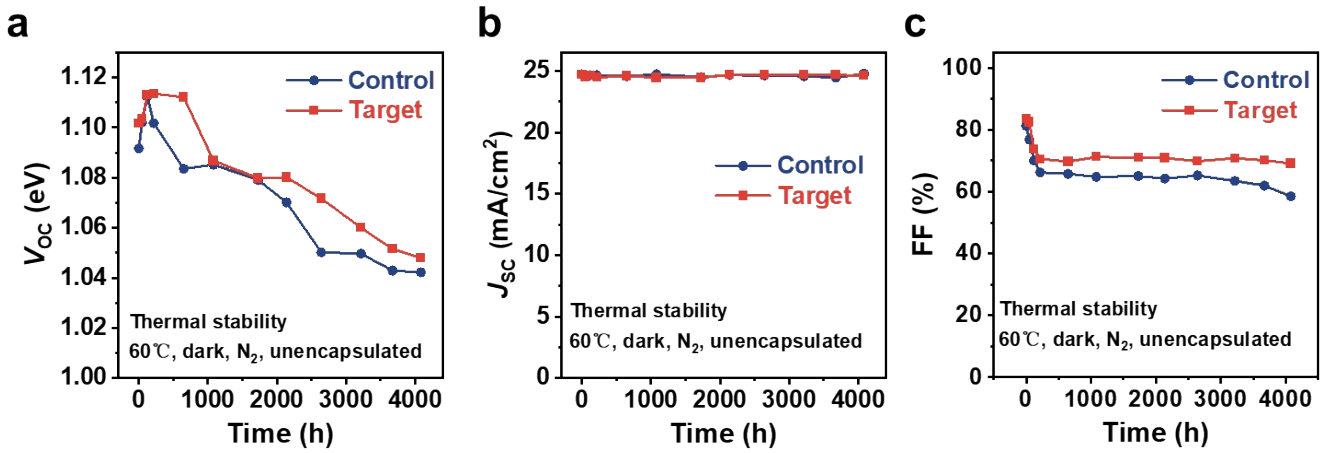

Supplementary Fig. 16. Distributions of V_{OC} (a), J_{SC} (b), FF (c) of control and target devices under continuously heating at 60℃ in N_2 atmosphere.

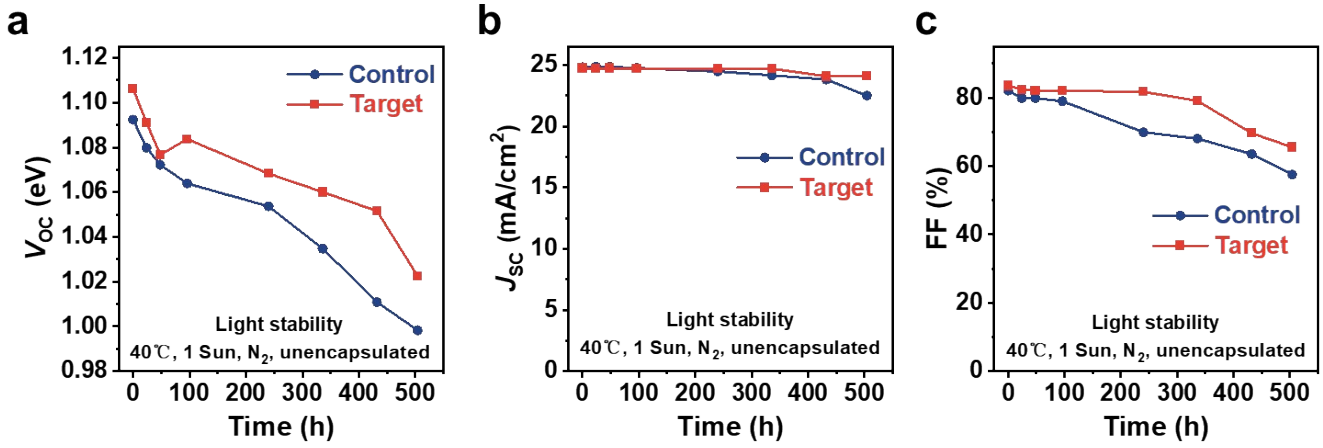

Supplementary Fig. 17. Distributions of V_{OC} (a), J_{SC} (b), FF (c) of control and target devices under under continuous one-sun illumination at 40 ± 5 °C in N_2 atmosphere.

Composition	Control (Glass/NiO_x)				Target (Glass/H_2O_2-NiO_x)			
	BE (eV)	Area	FWHM (eV)	Ratios	BE (eV)	Area	FWHM (eV)	Ratios
NiO	853.9	40454.42	1.21	1.00	853.9	34219.4	1.24	1.00
Ni_2O_3	855.4	55211.54	2.28	1.36	855.4	50423.28	2.37	1.47
NiOOH	856.5	42969.90	3.03	1.06	856.5	38485.00	3.31	1.12
Satelite	860.9	76960.77	3.63	1.90	861.0	66916.73	3.61	1.96
Satelite	864.0	13770.92	2.47	0.34	864.0	12704.15	2.61	0.37
Satelite	866.4	7504.51	2.24	0.19	866.6	6025.23	2.26	0.18

Supplementary Table 1 Peak fitting parameters of the Ni $2p_{3/2}$ core level spectra.

Supplementary Table 2 The fitting parameters of TRPL measurement of perovskite film based on NiO_x/SAMs and H_2O_2-NiO_x/SAMs substrate. The average decay time (τ_{ave}) were calculated according to the formula: $\tau_{ave} = (A_1\tau_1^2 + A_2\tau_2^2)/(A_1\tau_1 + A_2\tau_2)$.

	τ_1 (ns)	A_1 (%)	τ_2 (ns)	A_2 (%)	τ_{ave} (ns)
ITO	17.47	65.41	1372.07	442.78	1369.52
NiO_x	17.56	96.48	574.63	234.34	567.71
H_2O_2-NiO_x	12.73	111.46	396.78	209.10	390.33